Mem. S.A.It. Vol. 74, 737

Memorie della

Parametric nonlinear evolution of Alfvén waves in the fast solar wind

L. Del Zanna

Dipartimento di Astronomia e Scienza dello Spazio, Università degli Studi di Firenze, Largo E. Fermi 2, 50125 Firenze

Abstract. Alfvén waves are known to be the dominant modes in the turbulence spectrum in fast solar wind streams, but their evolution with heliocentric distance has not a clear explanation yet. Here the stability of monochromatic large-amplitude Alfvén waves is investigated via MHD numerical simulations. The nonlinear evolution of parametric decay seems to be a viable mechanism to explain the observed bahaviour.

1. Introduction

The low-frequency part of fluctuations spectra in high-speed and polar regions of the solar wind is known to be dominated by large-amplitude Alfvén waves propagating outwards (Belcher & Davis 1971), probably originated in coronal holes at the Sun, where the magnetic field is open and mainly unipolar. Fluctuations seen in slow solar wind streams (on the equatorial plane) evolve rapidly towards a classical Kolmogorov turbulent cascade, driven by velocity and magnetic shears ubiquitous there (Malara et al. 1992), while in polar regions, where these features are rare (at least on a large scale) the turbulence evolution is much slower: the spectrum has initially a smaller index, reaching values close to -5/3 only at large distances, and at the same time the prevalence of outward propagating modes decreases monotonically (Roberts et al. 1987). Moreover, this process seems to saturate at a certain distance (around 2.5 AU, from Ulysses data, Bavassano et al. 2000; see also Bavassano's contribution in these proceedings).

The origin of this residual turbulence evolution is still a matter of debate: incompressible fluctuations with an initial imbalance between outward and inward propagating modes should evolve in a way as to increase this imbalance, rather than to decrease it (*dynamical alignment*, Dobrowolny el al. 1980). The observed process was first supposed to be due just to overall solar wind expansion effects (e.g. Grappin & Velli 1996), but a promising alternative is provided by compressible wave-wave nonlinear interactions, namely parametric decay.

When an Alfvén wave propagates by keeping an overall constant magnetic field strength, regardless of its amplitude, the coupling to compressive perturbations leads to a decay of the mother wave in favour of a backscattered Alfvénic mode and of a steepening magnetosonic wave. Therefore the process *reduces* the initial Alfvénic imbalance, as needed. When com-

Send offprint requests to: L. Del Zanna
Correspondence to: ldz@arcetri.astro.it

pressive waves start to dissipate into shock fronts the resonance is lost and the decay saturates. This process is rather robust, since it occurs for a variety of wave amplitudes and plasma betas; in general the evolution in a low-beta plasma is faster but even in equipartition conditions, like in the solar wind, growth rates are reasonably high for sufficient wave amplitudes. In the present paper we summarize the results of MHD numerical simulations of monochromatic Alfvén waves in both parallel (Del Zanna et al. 2001, DZ1) and oblique (Del Zanna 2001, DZ2) propagation.

2. Parallel propagation

When Alfvén waves propagating along a main uniform field $\mathbf{B}_0$ are circularly polarized, the total field intensity is constant and these waves are exact solutions of the full MHD equations regardless of their amplitude. However, it is also well known that these solutions are actually unstable in the presence of small compressive fluctuations. After a transient period, the initial pump wave (with wave number k_0) decays into a sound-like compressive wave (with greater wave number k_c) and into a backward propagating Alfvén-like transverse mode (with wave number $k_t = -(k_c - k_0)$). In the small $\eta = B_\perp/B_0$ and $\beta = c_s^2/v_A^2$ limit, the linear dispersion relations for sound and Alfvén waves can be employed in the following resonance conditions

$$k_0 = k_c + k_t, \quad \omega_A(k_0) = \omega_s(k_c) + \omega_A(k_t), \quad (1)$$

yielding the unstable wave numbers and the linear growth rate γ as:

$$k_c \simeq 2k_0, \quad k_t \simeq -k_0; \quad \gamma \simeq \omega_0 \eta \beta^{-1/4}. \quad (2)$$

Here, like in DZ1 and DZ2, three sets of parameters are considered, with values appropriate for solar wind conditions near the Sun (A: $\eta = 0.2$, $\beta = 0.1$), intermediate (B $\eta = 0.5$, $\beta = 0.5$), and at the Earth's orbit (C $\eta = 1.0$, $\beta = 1.2$). The resulting growth rates are in all cases very similar ($\gamma \simeq 0.4$ for $k_0 = 4$).

In DZ1 the development of the parametric decay was studied via numerical simulations (using a high-order shock-capturing 3D-MHD code, Londrillo & Del Zanna 2000), for the three cases, in a periodic numerical box where the exact solution Alfvén wave with $k = k_0$ was initially set, together with a small (10^{-4}) density white noise to trigger the instability. Both the linear phase and the nonlinear saturation were followed by plotting the time histories of the density fluctuations, of the Elsässer energies $E^\pm$ and of the normalized cross helicity, defined by

$$\sigma = \frac{E^+ - E^-}{E^+ + E^-}, \quad E^\pm = < \frac{1}{2} |\mathbf{z}^\pm|^2 >, \quad (3)$$

where $\mathbf{z}^\pm = \delta\mathbf{v} \mp \delta\mathbf{B}$ ($\mathbf{z}^+$ is here the outgoing wave) and brackets indicate spatial averaging.

The results show that after the exponential growth of the daughter waves and of density fluctuations during the linear phase, there is a saturation when nonlinear steepening and heat dissipation occurs. Correspondingly r_A increases ($\sigma = (1 - r_A)/(1 + r_A)$ decreases) until it reaches a final constant value that appears to depend strongly on the plasma beta. In high-beta conditions an asymptotic balance between outward and inward modes is found, as observed with increasing heliocentric distance in the solar wind, while for low-beta conditions the cross helicity usually reverses its sign (the backscattered wave becomes the dominant mode) and sometimes even multiple decays are observed. Similar results are also found in 2-D and 3-D and even in non-periodic domains, confirming the robustness and universality of the parametric decay process.

3. Oblique propagation

All solar wind *in situ* data show clearly that Alfvénic magnetic field oscillations are never circularly polarized, as would be natural for parallel propagating Alfvén waves preserving $B \sim$ const, but rather show a spherical arc-type polarization, with the

tip of $\delta\mathbf{B}$ describing circular arcs (rotations are usually less than 180°) on the surface of an imaginary sphere with radius $B = |\mathbf{B}|$. According to Riley et al. (1996), who performed a systematic analysis by studying *Ulysses* fast-stream data in the ecliptic plane, up to 10% of Alfvénic modes are pure arc-polarized waves, meaning that the plane containing the maximum and intermediate variance directions remains fixed in time. The majority of the events was best explained by planar (1-D) arc-polarized Alfvén waves propagating obliquely to the background magnetic field and by embedded phase-steepened structures (rotational discontinuities: RDs). Arc polarization for large-amplitude oblique Alfvénic modes was first proposed by Barnes and Hollweg (1974) who showed, by performing a second-order expansion of the 1-D MHD nonlinear equations, that a monochromatic Alfvén wave which is initially linearly polarized develops another oscillatory component achieving arc polarization and $B^2 = \text{const}$. These predictions were investigated numerically via hybrid simulations by Vasquez and Hollweg (1996).

The first result that we show here is the total independence of the parametric decay process by the actual polarization of the mother wave. We take as initial condition an Alfvén wave in oblique propagation (k_0 is along z and B_0 makes an angle θ with it, with another component along y), given by

$$B_x = \eta B_0 \cos(k_0 z), \quad B_y = \sqrt{C^2 - B_x^2}, \tag{4}$$

where $C^2 = B_x^2 + B_y^2 = B^2 - {B_0}_z^2$ is the constant squared module of the transverse magnetic field and is obtained by imposing $< \delta B_y >= 0$, see DZ2 for details.

In Fig. 1 we plot the *rms* density fluctuations, the normalized cross helicity σ and the Elsässer energies $E^{\pm}$ (normalized to $E^{+}(0)$) for run A parameters and for $\theta = 30°$. Like in DZ1 multiple decays may be seen, at least in this low-beta case, where density fluctuations first increase and then saturate and where the dominant

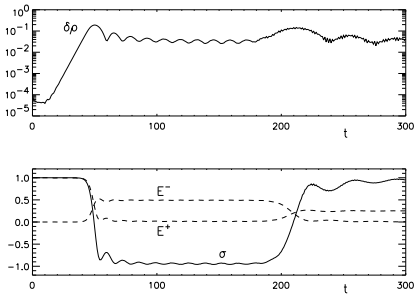

Fig. 1. Time histories of *rms* density fluctuations (top), normalized cross helicity σ and normalized Elsässer energies $E^{\pm}$. Parametric decay occurs twice, at $t = 50$ and $t = 210$. Here run A parameters with $\theta = 30°$ are employed.

wave looses about half of its energy at every instability saturation. Correspondingly, the cross helicity reverses its sign flipping between the ± 1 states for pure Alfvénic modes. The plots for run B and C are also very similar to those in DZ1 and are not reported here. The result that for $\beta \sim 1$ the asymptotic value of σ approaches zero after the first occurrence of the instability still holds (B: $\sigma = -0.3$, C: $\sigma = 0.2$).

Consider now the evolution of an oblique Alfvénic mode linearly polarized along the x direction but without any y component. This time B^2 is not constant and both a driven wave and magnetoacoustic waves, all with $k = 2k_0 = 8$, are expected to form (density noise at $t = 0$ is not needed, due to initial non-equilibrium). The driven wave, that travels at the same speed as the mother wave, tends to restore a $B^2 \simeq \text{const}$ condition by creating a B_y component in arc polarization. The situation may be seen in Fig. 2, where an almost exact arc with nearly constant total magnetic strength is achieved. The parameters are those of run B, $\theta = 30°$ and $t = 3\pi$. Note that the B_x profile has almost phase-steepened to a RD, although this is much more apparent for larger amplitudes.

Density fluctuations first increase very rapidly due to the ponderomotive force, but

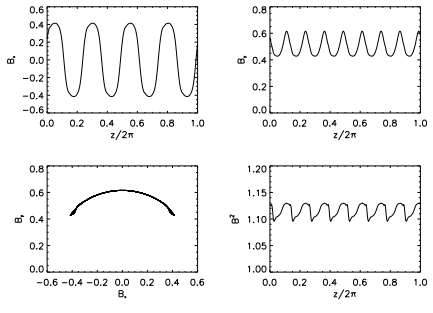

Fig. 2. Magnetic field components (B_z is constant and it is not shown), hodogram in the $B_x - B_y$ plane and B^2 for $t = 3\pi$. Here $\eta = \beta = 0.5$ and $\theta = 30°$.

soon steepen and dissipate through shock heating, causing the *rms* value to decrease. In general, for smaller β and larger η density fluctuations are larger, but also dissipate more rapidly. When this value reaches a noise level, the situation is very similar to that of the previous section because we have a traveling arc-polarized wave with an almost constant field strength: parametric decay finally sets in and the mother wave decays as usual. The linear growth rates are about the same as those of the corresponding case of initial arc polarization, just around 10% less because of a stronger wave amplitude decay: for example $\gamma = 0.120$ and $\gamma = 0.093$ are found for the cases corresponding to runs A and B.

4. Conclusions

Parametric decay is certainly a slow process in solar wind conditions, and both partial reflection due to Alfvén speed gradients or interaction with velocity shear layers are able to shape the turbulent spectrum in much shorter time-scales. However, this process seems to be able to explain rather naturally the evolution of the turbulent spectrum in the smooth polar wind, as described in the introduction. By taking our parameter sets A, B and C, that simulate different conditions from the outer corona to the Earth and for which the ratio $\gamma/\omega_0 \sim 5\%$ is constant (say it does not depend on the distance from the Sun), a wave with $P_0 \sim 10^4$ s will decay with a characteristic e-folding distance $d \sim (1/2\pi)(\gamma/\omega_0)^{-1} v_{\rm SW} P_0 \sim 0.2$ AU for $v_{\rm SW} \sim 800$ km/s, that has the correct order (it may be slightly larger when considering non-monochromatic waves or dispersive effects). Moreover, the *Ulysses* polar wind data by Bavassano et al. (2000) show that the Alfvénic ratio ceases to increase at 2.5 AU, its value being $r_A \sim 0.5 \Rightarrow \sigma = (1 - r_A)/(1 + r_A) \sim 0.3$, to be compared with our asymptotic value of $\sigma \sim 0.2$ for solar wind conditions. However, for more realistic and quantitative modeling, non-monochromatic wave trains, dispersion and radial expansion should be all included in future simulations.

References

Barnes A., Hollweg J.V., 1974, JGR 79, 2302

Bavassano B., Pietropaolo E., Bruno R., 2000, JGR 105, 15959

Belcher J.W., Davis Jr. L., 1971, JGR 76, 3534

Del Zanna L., Velli M., Londrillo P., 2001, A&A 367, 705 (DZ1)

Del Zanna, L., 2001, GRL 28, 2585 (DZ2)

Dobrowolny M., Mangeney A., Veltri P., 1980, PhRvL 45, 144

Grappin R., Velli M., 1996, JGR 101, 425

Londrillo P., Del Zanna L., 2000, ApJ 530, 508

Malara F., Veltri P., Chiuderi C., Einaudi G., 1992, ApJ 396, 297

Malara F., Primavera L., Veltri P., 2000, Phys. Plasmas 7, 2866

Riley P., et al., 1996, JGR 101, 19987

Roberts D.A., Goldstein M.L., Klein L.W., Matthaeus W.H., 1987, JGR 92, 12023

Vasquez B.J., Hollweg J.V., 1996, JGR 101, 13527